Nanoscale

PAPER

Check for updates

Targeted delivery of cytotoxic proteins *via* lipid-based nanoparticles to primary Langerhans cells†

Nowras Rahhal, [a,b,c] Mareike Rentzsch, [a,b,c] Saskia Seiser, [d]
Christian Freystätter,[e] Adelheid Elbe-Bürger [d] and Christoph Rademacher [*a,b]

Targeted delivery has emerged as a critical strategy in the development of novel therapeutics. The advancement of nanomedicine hinges on the safe and precise cell-specific delivery of protein-based therapeutics to the immune system. However, major challenges remain, such as developing an efficient delivery system, ensuring specificity, minimizing off-target effects, and attaining effective intracellular localization. Our strategy utilizes lipid-based nanoparticles conjugated with a glycomimetic ligand. These nanoparticles selectively bind to langerin, a C-type lectin receptor expressed on Langerhans cells in the skin. We opted for cytotoxic proteins, namely cytochrome c and saporin, as model proteins to showcase the potential of delivering intact proteins to Langerhans cells. These proteins are recognized for their ability to induce apoptosis upon entry into the cytosol. We observed specific killing of cells expressing langerin *in vitro*, and in primary Langerhans cells isolated from mouse and human skin *ex vivo* with minimal off target effects. By delivering functional proteins within lipid nanoparticles to Langerhans cells, our approach offers new potential to deliver effective therapeutics with minimal side effects.

Introduction

The therapeutic potential of cytosolic delivery of macro-molecules, such as DNAs, RNAs, and proteins, is immense, offering new treatments for a wide array of diseases from genetic disorders to cancer.[1] However, clinical translation of such therapeutics is challenged amongst other factors by the specificity of delivery to defined cells with limited off-target effects, overcoming membrane barriers, ensuring escape from endosomal entrapment, and directing precise subcellular localization.[2] Recent studies in the field of nanomedicine have highlighted the potential of intracellular delivery, exemplified by the clinical endorsement of RNA delivery for gene silencing (*e.g.*, Onpattro®) and COVID-19 vaccines.[3] Central to these achievements is the utilization of nanocarriers like lipid-based nanoparticles.[4,5] Although prior studies have demonstrated

the potential application of lipid-based nanoparticles for intra-cellular protein delivery,[6–8] challenges persist due to unspecific uptake of the particles, low endosomal escape and the inherent instability of proteins, hampering further advancement.[9]

The use of liposomes for protein delivery began with the encapsulation of lysozyme,[10] followed by the delivery of proteins such as β-glucuronidase[11] and β-galactosidase.[12] Recent studies have extended this approach to include lipid nanoparticles (LNPs) tailored with cationic or ionizable lipids for delivering anti-cancer agents,[13,14] cytotoxic proteins for cancer treatment,[15–18] and gene editing proteins like CRISPR/Cas9.[19] Despite these advancements, enhancing delivery efficiency, therapeutic outcomes and targeting specificity remains imperative.

We previously reported the development of a small molecule glycomimetic targeting ligand that specifically binds to the C-type lectin (CLR) langerin (CD207) that is expressed on Langerhans cells (LCs).[20,21] Residing in the epidermis, LCs are frontline sentinels that play a crucial role in identifying pathogens *via* langerin and other pattern recognition receptors (PRRs), leading to endo/lysosomal antigen processing and promoting a potent adaptive immune cascade *via* both T cell and B cell activation.[22–25,49] This glycomimetic targeting ligand has proven versatile and has been used for the specific delivery of liposomal formulations as well as direct conjugation of the ligand to protein carriers.[26]

a Department of Pharmaceutical Sciences, University of Vienna, Vienna, Austria
b Department of Microbiology, Immunology and Genetics, University of Vienna, Max F. Perutz Labs, Vienna, Austria
c Vienna Doctoral School of Pharmaceutical, Nutritional and Sport Sciences, University of Vienna, Vienna, Austria
d Department of Dermatology, Medical University of Vienna, Vienna, Austria
e Department of Plastic and Reconstructive Surgery, Medical University of Vienna, Vienna, Austria
†Electronic supplementary information (ESI) available. See DOI: https://doi.org/10.1039/d4nr03638g

In this study, lipid-based nanoparticles of both liposomes and LNPs were utilized to encapsulate cytotoxic proteins, serving as model proteins, cytochrome c (Cyt C) and saporin. The aim was to induce apoptosis in langerin-expressing cells, demonstrating effective cytosolic protein delivery. To assess the specificity and efficacy of our cytotoxin-LNP system, we initially employed a langerin-expressing model cell line. Subsequently, we extended our investigation to primary LCs obtained from both mouse and human epidermal cell suspensions. Our results demonstrated a remarkable targeting specificity and efficacy towards LCs compared to other non-targeted cells. This approach effectively addresses the hurdles associated with intracellular delivery of large proteins thereby presenting a promising avenue for treating diseases necessitating precise subcellular delivery.

Results and discussion

Two distinct lipid-based nanoparticle systems were prepared using microfluidic techniques. Utilizing a staggered herringbone structure design, the cytotoxic proteins were passively loaded into the lipid-based nanoparticles.[27,28] We employed the ionizable lipid Dlin-MC3-DMA (MC3), which was used in the FDA-approved drug Onpattro for LNPs (DiLn-MC3-DMA: Chol:DSPC:DSPE-PEG), and similarly DSPC:Chol:PEG of Doxil were used for liposomes. Capitalizing on the strengths profile of both delivery systems as the earliest FDA-approved and most studied systems in literature with distinct intracellular trafficking pathways.[29] The prepared lipid-based nanoparticles loaded with cytotoxic proteins were characterized using dynamic light scattering and display average sizes of 139 ± 33 nm and a net negative charge at pH 7.4 (Table S1†). The protein encapsulation was assessed after dialysis of the nanoparticles using BCA protein quantification assay. We observed that only less than 7% of the initial protein concentration for Cyt C and

around 30% for saporin prior to the formulation was loaded into the nanoparticles.[30,31] Other reports in literature using passive loading of proteins with microfluidic techniques reported similar values on encapsulation efficiencies of 2–4% for BSA in liposomes. Despite having two different lipid-based nanoparticle systems, LNPs and liposomes, with different characteristic features on the molecular level, there were no significant differences in size, charge and loading (Table S1†).

Cyt C targeted LNPs exhibit selective cytotoxicity towards human langerin-expressing cells

To evaluate cell viability, we initially employed lipid-based nanoparticles loaded with Cyt C, a protein known to induce apoptosis when translocated to the cytoplasm.[32] The formulations were tested on the established Raji cell line that expresses the langerin receptor (Fig. S1†).[20] We evaluated the uptake of LNPs conjugated with the targeting ligand (t LNPs) and compared them to non-targeted particles (nt LNPs) (Fig. 1a). When the glycomimetic targeting ligand was covalently attached to the nanoparticles, we observed a high cytotoxic effect of LNPs loaded with Cyt C (Fig. 1b). This reduction in cell viability was only observed in human langerin-expressing cells, underscoring the specificity of our targeting approach for the human receptor (Fig. 1b). The high specificity of our targeting mechanism compensates for the relatively low encapsulation efficiency and enables effective outcomes even at reduced protein concentrations. In addition, as anticipated, pre-incubation of cells with mannan, a mannose-rich polysaccharide derived from *Saccharomyces cerevisiae* and a known inhibitor of langerin,[33] prevented apoptosis following LNP treatment (Fig. 1a). Notably, free Cyt C, even at ten-fold higher concentration, failed to induce cell death (Fig. S2†). This corroborates that free Cyt C does not permeate the cell membrane owing to its large and complex biomolecular properties,[34] which constitutes a major problem for the intracellular delivery of proteins.[2] Additionally, empty targeted (et) LNPs did not
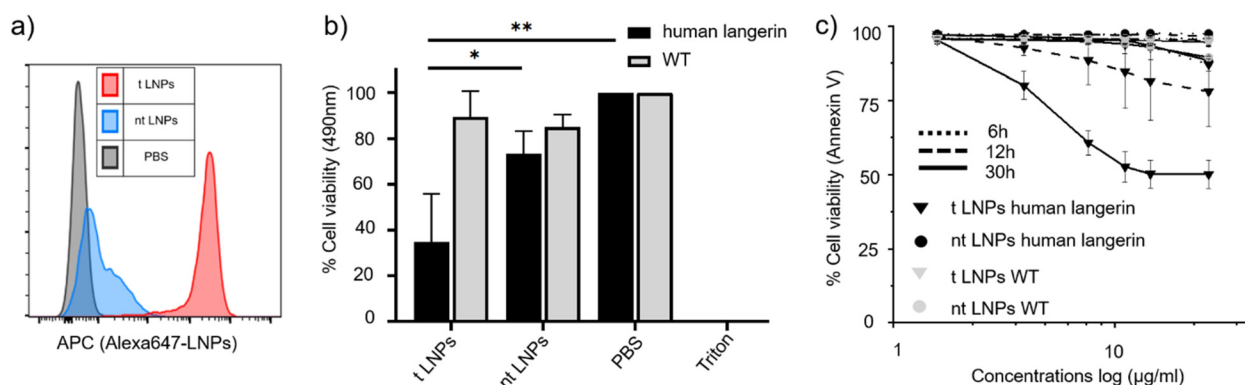
Fig. 1 *In vitro* cell proliferation/viability assays on wild-type (WT) and human langerin (hL) expressing Raji cells. (a) Flow cytometric analysis of LNP uptake into WT and hL Raji cells after 30 hours of incubation shows a specific uptake to hL-expressing Raji cells. (b) Viability of WT and hL Raji cells after treatment with t and nt LNPs encapsulating Cyt C (25 µg mL^{-1} of the protein loaded in the nanoparticles) for 24 hours. 0.1% Triton solution was used as a positive control to cause robust cell lysis. Error bars represent the standard deviation (SD) of the mean for three independent experiments (*$p < 0.05$, **$p < 0.01$). (c) Flow cytometric apoptotic analysis of Raji cells using Annexin V staining at three-time points and Cyt C concentrations from 1 µg mL^{-1} to 26 µg mL^{-1} of protein loaded in the nanoparticles. Error bars are presented as mean SD from three independent measurements.

exhibit cytotoxicity, confirming the role of Cyt C and excluding LNP-induced effects (Fig. S2†). In contrast, alongside LNPs we also compared the delivery efficiency of liposomal formulations to deliver Cyt C to the cytosol. Herein, liposomes failed to induce cytotoxicity in comparison to LNPs (Fig. S2†). This may be attributed to a critical step of intracellular cytosolic delivery called the endosomal escape. The lack of cytotoxicity in the liposomal formulation could be due to the lack of an ionizable lipid component. Without this component, Cyt C within the liposomal system ends up in the lysosome and is unable to reach its cytosolic intracellular target and thus further induce apoptosis.[35] Researchers emphasize that ionizable and cationic lipids are crucial for facilitating cargo endosomal escape in such delivery systems.[36]

To further optimize the LNP formulation, we investigated the impact of two modifications. First, we replaced cholesterol with β-sitosterol, a structural analogue reported to enhance mRNA translation efficiency by increasing the endosomal escape.[37,38] Notably, LNPs containing β-sitosterol exhibited similar cytotoxicity to Raji cells as cholesterol-based formulations (Fig. S3†), indicating minimal impact on the overall apoptotic effect of the Cyt C protein. Second, we substituted the ionizable lipid DLin-MC3-DMA (MC3) with the synthetic lipid COATASOME SS-EC (SS-EC), which has been reported to exhibit high efficacy in targeting macrophages,[39,40] and therefore was used here, since LCs were reported of having macrophage–dendritic-like features.[34] However, these LNPs did not induce apoptosis in Raji cells as expected (Fig. S3†). This observation might be attributed to the chemistry of the SS-EC lipid; its disulfate bond facilitates thiol production within the acidic endosomal environment. Since thiols act as reducing agents, they could potentially mitigate the apoptotic function of the Cyt C protein.[41] Overall, modifying the LNP formulations to include β-sitosterol has been proven to maintain cytotoxic efficacy. However, substituting MC3 with SS-EC lipid, despite aiming to increase efficacy, did not result in the anticipated apoptotic effect.

Next, we performed Annexin V-based flow cytometric apoptotic analysis on Raji cells to assess the early apoptotic marker phosphatidylserine. LNPs loaded with Cyt C (1–26 μg mL^{-1} of the protein loaded in the nanoparticles) were tested at 6, 12, and 30 h time intervals. A dose- and time-dependent decrease in cell viability was observed exclusively for the targeted LNPs in langerin-expressing cells (Fig. 1c), whereas WT cells exhibited minimal apoptosis when exposed to either t or nt LNPs. This underscores the specificity of the targeted delivery system and its langerin-mediated uptake.

These flow cytometric analyses confirm our previous MTS assay results and provide additional insight into the time-dependent efficacy of our targeted nanoparticle formulation in inducing apoptosis in langerin-expressing cells. The targeted LNPs demonstrated their intended cytotoxicity, consistent with our design to selectively deliver their apoptotic cargo to langerin$^+$ cells. Consequently, we proceeded to test our formulations on primary LCs from both mouse and human skin.

## Saporin-loaded targeted LNPs deplete primary LCs from human langerin DTR mice

We expanded our study to include primary LCs from mouse skin. LCs are crucial for internalizing pathogens via langerin and cross-presenting exogenous antigens to trigger T cell responses.[23,42] Given their strategic location in the skin, LCs are ideal targets for cutaneous vaccines aimed to elicit robust immunity, a process that often faces challenges in precise and efficient delivery of antigens and adjuvants. Additionally, in LC histiocytosis, lesions are predominantly composed of langerin$^+$ myeloid progenitor cells, highlighting the need for targeted delivery of therapeutics to mitigate adverse effects.[43] We used saporin protein, a plant-derived protein from *Saponaria officinalis*, which is known as a ribosome-inactivating protein with high cytotoxic potency.[44] The high therapeutic potential of saporin is limited by its poor cell permeability and unclear intracellular trafficking mechanism.[45] Our aim was to demonstrate the adaptability of our delivery system to different cargos and to show *ex vivo* potency against primary LCs.

Accordingly, we prepared epidermal single cell suspensions from the skin of DTR C56BL/6 mice, which express the human langerin receptor on LCs.[46] In these cell suspensions, the human langerin receptor is found on LCs.[47] Epidermal cell suspensions were incubated with saporin-loaded LNPs at a concentration of 30 μg mL^{-1} of the protein loaded in the nanoparticles for 16 hours. For the flow cytometric analysis, LCs were identified within the epidermal skin suspension as single, viable, MHC class II$^+$ cells (Fig. S4†). We observed that targeted saporin-loaded LNPs induced a significant depletion of LCs. In contrast, nt LNPs LCs showed only minimal depletion of LCs (Fig. 2a and d). In addition, LCs showed high uptake signals of AF647dye-LNPs when the particles incorporated our glycomimetic ligand (Fig. 2b). In contrast, the nt LNPs showed only minimal depletion of LCs. Importantly, analysis of other cell populations in the epidermal cell suspension showed negligible apoptosis of non-target cells, suggesting minimal off-target effects (Fig. 2c). This is crucial in the development of highly selective cytotoxic therapies. The remarkable specificity observed in the depletion of primary LCs confirms the effective cytosolic delivery of intact functional proteins to these cells using our targeted LNP system.

Cyt C-loaded targeted LNPs deplete primary LCs from human skin

Next, to extend our findings to human cells, we investigated the effect of Cyt C-loaded LNPs at a concentration of 25 μg mL^{-1} of the protein loaded in the nanoparticles on primary LCs in epidermal cell suspensions derived from human skin. Following a 24-hour incubation with LNPs, we analyzed cell viability via flow cytometry and identified single cells, specifically langerin$^+$ cells (Fig. S5†). Consistent with the murine data (Fig. 2), significant apoptosis in primary LCs was observed exclusively in samples treated with t LNPs (Fig. 3a and d). Nanoparticle uptake was tracked using Alexa647 conjugated to DSPE-PEG in our formulations. LCs displayed a markedly high
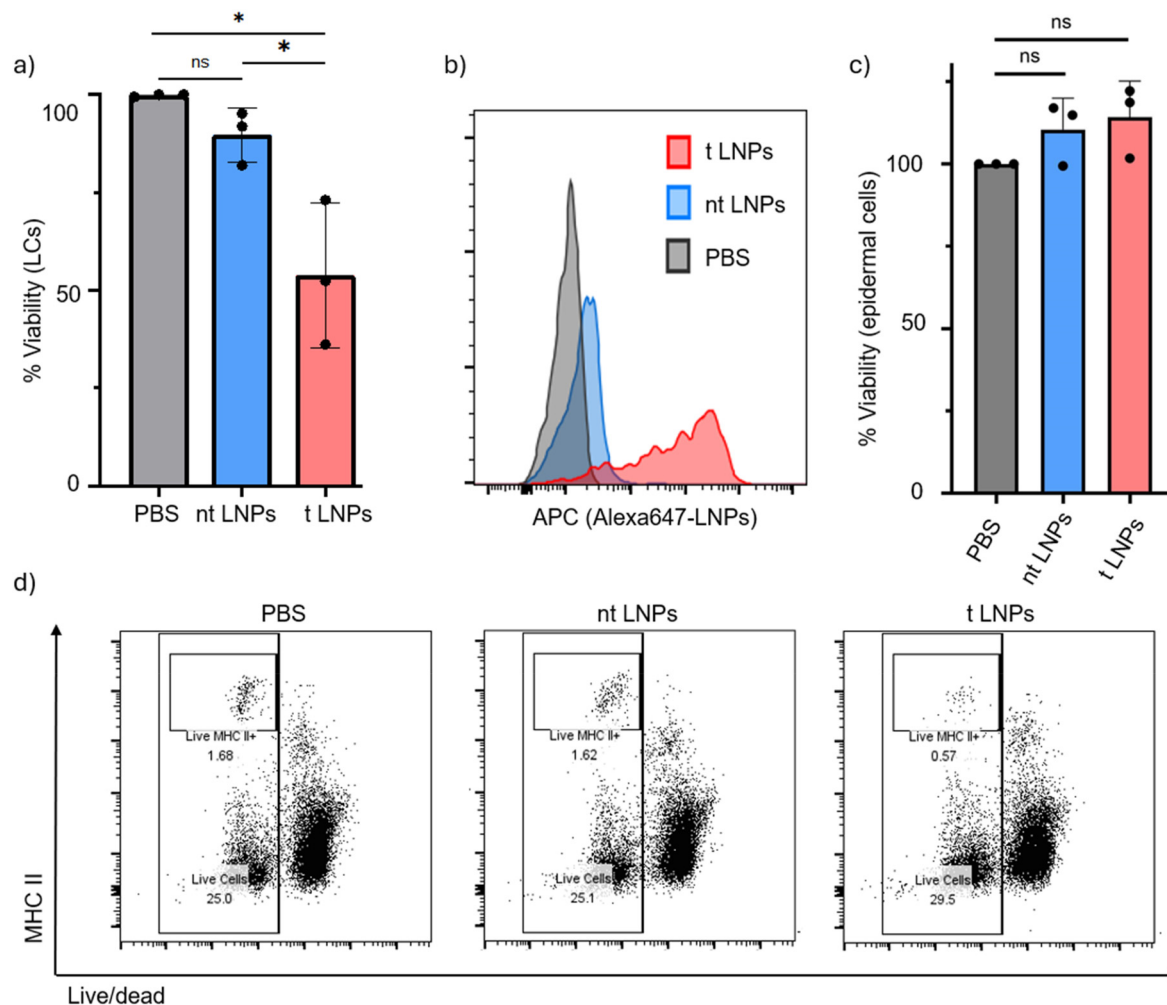
Fig. 2 *Ex vivo* cytotoxic delivery of saporin-LNPs to primary LCs isolated from the skin of human langerin DTR mice. (a) LCs viability normalized to PBS after treatment with the targeted (t) LNPs (red), non-targeted (nt) LNPs (blue) and PBS control (grey). Statistical significance is denoted according to an independent two-tailed unpaired Student's *t*-test where the error bars represent the mean standard deviation (SD) of three independent biological experiments (*$p < 0.05$, ns: not significant). (b) Representative histogram overlays show LCs uptake of Alexa647-labeled LNPs. (c) Total viability of all epidermal cells, normalized to PBS, after treatment with t and nt LNPs and PBS control. Statistical significance is denoted according to an independent two-tailed unpaired Student's *t*-test where the error bars represent the mean SD of three independent biological experiments. (d) Dot plots of gating for viable LCs: viable, MHCII^{+} cells.

uptake of t LNPs, underscoring once more the specificity of our delivery system (Fig. 3b). Importantly, neither t nor nt LNPs induced significant cytotoxicity in the broader population of viable epidermal cells, mainly keratinocytes, when compared to the PBS control (Fig. 3c). The specificity in inducing apoptosis in LCs while sparing other cell types underscores the versatility of our system and highlights the potential clinical relevance of our nanoparticle formulations.

Experimental

### Cell line and culture conditions

Raji cells, a human B lymphocyte cell line, were previously stably transduced with human langerin (Fig. S1†).[20] Raji cells were cultured in RPMI medium supplemented with 10% v/v

fetal calf serum (FCS) (Cytiva) and a 100 U mL^{-1} penicillin–streptomycin antibiotic mixture (Thermo Fisher Scientific). Cell densities were maintained between $0.25–2 \times 10^6$ cells per mL. For cell splitting, cells were centrifuged at 400g for 5 minutes (Heraeus Megafuge 8R, Thermo Fisher Scientific), the supernatant was aspirated and the cells were resuspended in fresh medium every 2–3 days. Cells were monitored routinely with a light microscope and incubated in 10 cm round flat-bottom plastic culture dishes (Corning) at 37 °C and 5% CO$_2$ (Cooling Incubator KB series, Binder GmbH).

Transgenic mice

Previously generated C57Bl/6 mice express the human langerin receptor and the diphtheria toxin receptor (DTR) exclusively in LCs.[46] The study included mice from both sexes that were kept under pathogen-free conditions. All mice used for the experi-
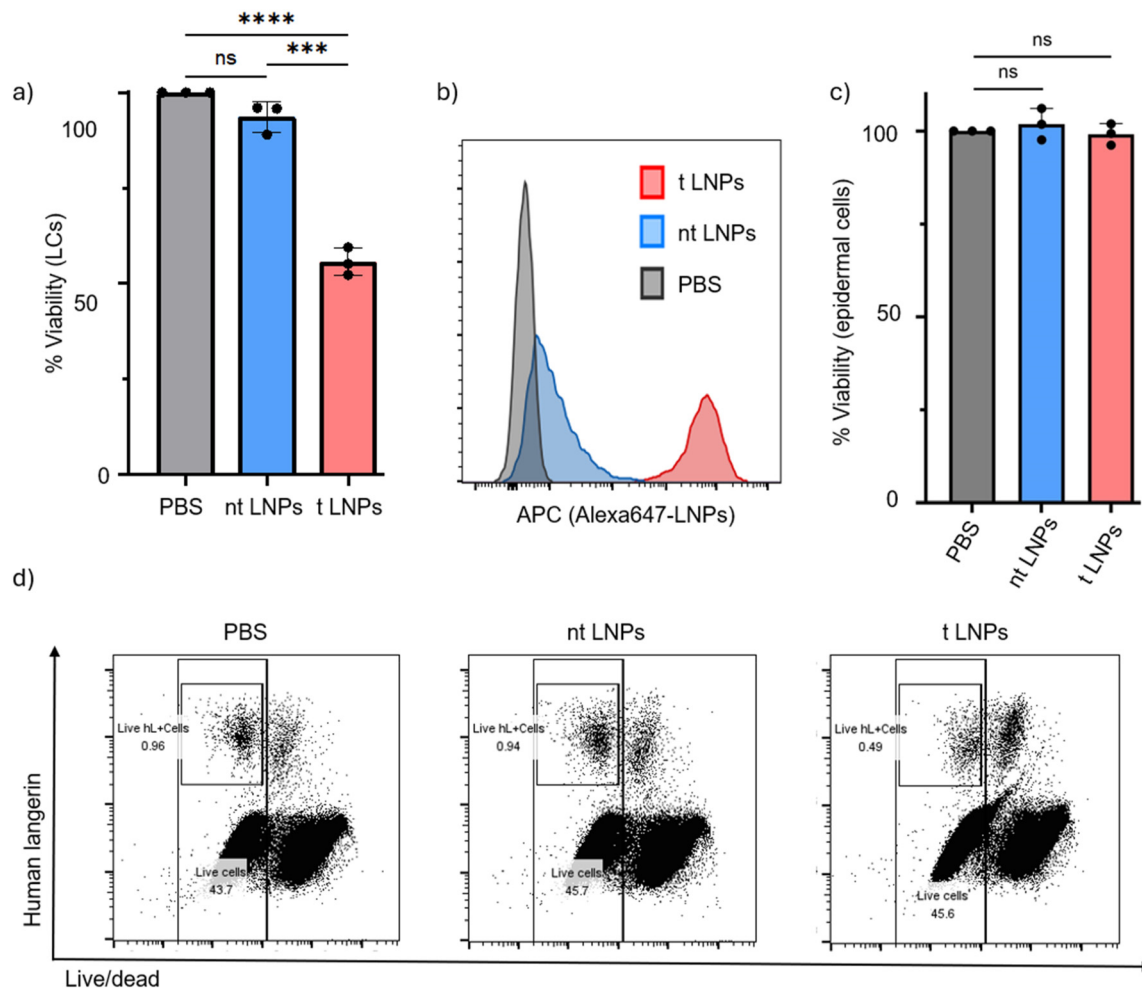
Fig. 3 *Ex vivo* cytosolic delivery of Cyt C-LNPs to primary human LCs derived from adult human skin. (a) Epidermal cell suspensions from three donors (males, females, age range between 37–43 years, *n* = 3) were prepared, LC viability normalized to PBS after treatment with the targeted (t) LNPs (red), non-targeted (nt) LNPs (blue) and PBS control (grey). Data was assessed *via* flow cytometry. Statistical significance is denoted according to an independent two-tailed unpaired student *t*-test where error bars represent the mean standard deviation (SD) of three independent experiments (**** $p < 0.0001$, *** $p < 0.001$, ns = not significant). (b) Representative histogram overlays showing the uptake of Alexa647-labeled LNPs by LCs. (c) Total viability of epidermal cell populations, normalized to PBS, after treatment with t LNPs, nt LNPs, and PBS control. Statistical significance is denoted according to an independent two-tailed unpaired Student's *t*-test where the error bars represent the mean SD of three independent biological experiments indicating not-significant (ns) differences compared to PBS. (d) Dot plots of gating for viable LCs: viable, human langerin^{+} cells.

mental procedures were aged 3 to 5 months and were bred internally.

Ethics statement and human skin donors

Skin samples from anonymous healthy adult donors (males, females, age range between 37–43 years, *n* = 3) were obtained 1–2 hours after plastic surgery procedures at the General Hospital of Vienna (Allgemeines Krankenhaus Wien, AKH). In accordance with ethical practices, each donor was informed about the nature and scope of the research, and written consent was obtained. This process was conducted according to the principles of the Declaration of Helsinki as well as in compliance with the ethics approval granted by the ethics committee of the Medical University of Vienna (ECS.1969/2021).

Single cell suspension of mouse epidermal cells

After euthanasia, mice were epilated, and skin samples were harvested from the abdomen, back and ears and transferred to Petri dishes. The subcutaneous adipose layer was carefully scraped off from the dermal side of abdominal and back skin samples using a scalpel. The skin was sectioned into connected fragments. Enzymatic dissociation was performed using 10 mL of 0.6% trypsin PBS (Sigma-Aldrich) at 37 °C for 30 min. To stop trypsinization, the skin was transferred to 10 mL of FBS (Cytiva), and the epidermis was carefully peeled off. The isolated epidermal compartment was transferred to complete medium and mechanically disrupted with forceps. Cells were further minced with scissors and incubated at 37 °C with agitation for an additional 15 min. After sequential filtration through 100 μm cell strainers and another filtration

with 40 μm cell strainers (Greiner Bio-One), cells were washed with PBS at every step and centrifuged at 400*g* for 5 min at 4 °C. Cell counts were performed to prepare cells for downstream applications. The cells were then seeded in a 96-well plate at a density of 1×10^6 per well.

Single cell suspension of human epidermal cells

Human skin grafts were cut using a dermatome (Zimmer Biomet) to a thickness of 0.5 mm. The samples underwent enzymatic digestion in RPMI medium supplemented with 1% penicillin–streptomycin (Gibco) and 2.4 U mL^{-1} dispase II (Roche) and 0.05% trypsin (Sigma) at either 4 °C overnight or 37 °C for 3 hours at 37 °C. The epidermal layer was carefully separated from the dermis using tweezers, minced into small pieces, and further digested in 0.05% trypsin (Sigma) for 20 min at 37 °C. The cell suspension was filtered through 100 μm and 40 μm cell strainers respectively. The cells were then spun down at 300 g for 5 min at 4 °C, resuspended in RPMI supplemented with 1% penicillin–streptomycin and 10% FCS and then counted for subsequent experimental steps. Cells were then seeded in a 96-well plate at 1×10^6 per well.

Lipid-based nanoparticles preparation

The human langerin targeting ligand (hLL) and Alexa Fluor™ 647 (Alexa-647) Succinimidyl Ester (Invitrogen™, ThermoFisher Scientific) were conjugated *via* amide coupling to DSPE-PEG (NOF CORPORATION) as previously described (Fig. S6†).[21] Liposomes and LNPs were prepared by mixing two phases, an organic phase and an aqueous phase using a syringe pump (Pump 33 Dual Drive System Syringe Pump, Harvard Apparatus) in an own custom-made, S-shape and consist of multiple herringbone structure cycles microfluidic device (Polydimethylsiloxane (PDMS)) (Wunderlichips GmbH).

The composition of LNPs was derived from the Onpattro® formulation consisting of 50 mol% Dlin-MC3-DMA (Medkoo Biosciences), 38.5 mol% Cholesterol (Sigma Aldrich), 10 mol% 1,2-distearoyl-*sn-glycero*-3-phosphocholine DSPC (NOF CORPORATION), 1.35 mol% 1,2-distearoyl-*sn-glycero*-3-phosphoethanolamine-poly(ethylene glycol) SUNBRIGHT DSPE-020CN (NOF CORPORATION), or DSPE-PEG-ligand and 0.15 mol% conjugated DSPE-PEG-A647. If not mentioned otherwise, all formulations included the dye.

Liposomal formulations as derived from the Doxil® formulation, with 57 mol% DSPC, 38.5 mol% Cholesterol, 4.85 mol% DSPE-PEG2K or 3.5 + 1.35 mol% DSPE-PEG2K DSPE-PEG-ligand and 0.15 mol% conjugated DSPE-PEG-A647.

The organic phase contained the lipids (5 mM) in ethanol 100% (Sigma Aldrich) and the aqueous phase contained the protein in either PBS buffer or sodium acetate buffer (Invitrogen, ThermoFisher Scientific, USA) (50 mM) receptively for liposomes or LNPs. The initial protein concentrations used prior to mixing were 1 mg mL^{-1} for Saporin protein (Sigma-Aldrich) and 2.5 mg mL^{-1} for cytochrome c from bovine heart (Sigma-Aldrich). A dual syringe pump (Pump 33 Dual Drive System Syringe Pump, Harvard Apparatus) was loaded with two syringes (Braun-Injekt®) containing dissolved lipids in

ethanol at 5 mM concentrations, and the protein was dissolved in the buffer in the other. The pump was used to inject the two phases at a flow rate ratio (FRR) of organic : aqueous 1 : 4 and a total flow rate of 300–500 μL per minutes. After mixing, the product was collected from the outlet. Following the formulation process, the LNPs and liposomes were dialysed with 100 kDa Spectrum™ Dialysis Membrane Tubing (FisherScientific) or SPECTRA/POR Micro Float-A-Lyzer cut-off MWCO 100 kDa (dDBiolab) overnight with ×2000 volume of buffer (PBS, pH 7.4). The resulting particles were stored at 4 °C until further processing.

Nanoparticle characterization

The mean hydrodynamic diameter (*z*-average), zeta potential, and polydispersity index (PDI) (Table S1†) were measured using a Zetasizer Pro (Malvern Panalytical Ltd). Dynamic light scattering with a backscatter measurement was performed in UV transparent cuvettes (Sarstedt, Inc.), with a material refractive index (RI) of 1.45 and an absorption of 0.001 at temperature of 25 °C.

Additionally, the protein content in the lipid-based nanoparticles was quantified using the Micro BCA Bicinchoninic acid assay (Pierce BCA Protein Assay Kit, Sigma Aldrich). Briefly, samples were incubated with 25 μL of unknown samples and 200 μL of the working reagent at room temperature for up to two hours. Subsequent absorbance readings were taken using a plate reader to determine protein concentrations (Dynex Technologies).

MTS cytotoxicity assay and Annexin V staining of Raji cells

The anti-proliferative effect of various formulations was evaluated using a modified MTS assay (3-(4,5-dimethylthiazol-2-yl)-5-(3-carboxymethoxyphenyl)-2-(4-sulfophenyl)-2*H*-tetrazolium) (Cell Proliferation, Colorimetric, Abcam). Initially, the cells were plated in 96-well plates at 5×10^4 cells per well and treated with the designated lipid-based nanoparticle concentrations. Post 22 h incubation, 20 μL of MTS solution was added to each well, followed by a 2 h incubation at 37 °C. As a positive control for cell death, cells were exposed to Triton X-100 0.1% (10 μL). The absorbance was read at 490 nm using a plate reader (Agilent BioTek EPOCH2TS).

For apoptosis detection *via* Annexin V staining, the treated cells were seeded at 5×10^4 cells per well. After incubation for 6, 12 and 30 h, cells were centrifuged at 400*g* for 5 min, washed with PBS and stained with Annexin V-FITC (Miltenyi Biotec) in Annexin binding buffer, followed by a 20 min incubation on ice. After adding 100 μL of Annexin buffer to each well, samples were analyzed using flow cytometry (Cytoflex S, Beckman Coulter).

Staining for epidermal cell suspensions

Following lipid-based nanoparticle incubation for 18–24 h, epidermal cells isolated from mice and humans were washed with PBS and centrifuged at 400*g* for 5 min at 4 °C. First, cell viability was assessed using the "LIVE/DEAD™ Fixable Yellow Dead Cell Stain" (ThermoFisher Scientific). For extracellular

staining, cells were fixed using a fixing reagent "BD Cytofix/Cytoperm™ Fixation/Permeabilization Kit" (BD bioscience), followed by staining with an anti-CD207 antibody (Miltenyi Biotec), according to the manufacturer's instructions. Epidermal cells from mice were additionally labeled with an anti-mouse I-A/I-E monoclonal antibody for the identification of MHC class II (Biolegend, PE/Dazzle™) in PBS buffer supplemented with 10% BSA and 0.5 M EDTA (Sigma-Aldrich). After a final PBS wash, flow cytometric analysis was conducted on a Cytoflex S (Beckman Coulter). All handling was done with a multichannel pipette. LCs were identified as viable, MHC-II$^+$ or langerin$^+$ cells (Fig. S4 and S5†). Data analysis and visualization were performed on Flowjo, GraphPad Prism and Origin software.

Conclusion

Protein-based therapeutics hold significant promise for cancer treatment, yet their clinical advancement is impeded by critical delivery challenges. These include limited stability within the bloodstream, insufficient ability to penetrate cells, and a propensity for rapid uptake by the liver.[48] In this study, we showed the delivery of intact proteins to LCs using LNPs. Our LNPs, guided by the glycomimetic ligand and encapsulated with cytotoxic proteins, selectively induced apoptosis in langerin-expressing cells. The experiments were conducted on model cell lines and primary LCs derived from mouse and human epidermal cell suspensions, showing promising results for conditions such as LC histiocytosis.[43] Targeted delivery to LCs, which are immune cells residing in the epidermis could facilitate the use of lower therapeutic doses. This aligns with minimally invasive administration methods and enhances patient compliance. Ongoing studies aim to further elucidate the efficacy and safety of our targeted approach *in vivo*.

Author contributions

C. R., N. R. and M. R. designed the research. N. R. performed the experiments. C. R. and N. R. analyzed the data. C. F., S. S. and A. E.-B. provided the human skin explants. S. S. and N. R. prepared the human skin single cell suspension. N. R. and C. R. wrote the manuscript. A. E.-B., S. S. and M. R. edited the manuscript. C. R. provided, funding, conceptualization, project administration and supervision.

Data availability

To whom it may concern:

Data for this article, including MTT assay (xls files) and flow cytometry (fcs files) data are available at DYRAD, **https://doi.org/10.5061/dryad.4qrfj6qkd**.

Patient data from which skin samples were derived, cannot be made available since such data was not exchanged following the informed consent of the patient.

Conflicts of interest

C. R. is co-founder, advisor, and shareholder of Cutanos GmbH, a company that is working on the commercialization of a glycomimetic-based targeting of Langerhans cells.

Acknowledgements

References

1 S. Y. Chen, *et al.*, Recent advances in the intracellular delivery of macromolecule therapeutics, *Biomater. Sci.*, 2022, **10**(23), 6642–6655.

2 S. Le Saux, *et al.*, Nanotechnologies for Intracellular Protein Delivery: Recent Progress in Inorganic and Organic Nanocarriers, *Adv. Ther.*, 2021, **4**(6), 2100009.

3 L. R. Baden, *et al.*, Efficacy and Safety of the mRNA-1273 SARS-CoV-2 Vaccine, *N. Engl. J. Med.*, 2021, **384**(5), 403–416.

4 A. Akinc, *et al.*, The Onpattro story and the clinical translation of nanomedicines containing nucleic acid-based drugs, *Nat. Nanotechnol.*, 2019, **14**(12), 1084–1087.

5 E. Rohner, *et al.*, Unlocking the promise of mRNA therapeutics, *Nat. Biotechnol.*, 2022, **40**(11), 1586–1600.

6 Z. Gu, *et al.*, Tailoring nanocarriers for intracellular protein delivery, *Chem. Soc. Rev.*, 2011, **40**(7), 3638–3655.

7 J. A. Pachioni-Vasconcelos, *et al.*, Nanostructures for protein drug delivery, *Biomater. Sci.*, 2016, **4**(2), 205–218.

8 S. B. Ebrahimi and D. Samanta, Engineering protein-based therapeutics through structural and chemical design, *Nat. Commun.*, 2023, **14**(1), 2411.

9 F. Moncalvo, M. I. Martinez Espinoza and F. Cellesi, Nanosized Delivery Systems for Therapeutic Proteins: Clinically Validated Technologies and Advanced Development Strategies, *Front. Bioeng. Biotechnol.*, 2020, **8**, 89.

10 G. Sessa and G. Weissmann, Incorporation of lysozyme into liposomes. A model for structure-linked latency, *J. Biol. Chem.*, 1970, **245**(13), 3295–3301.

11 L. D. Steger and R. J. Desnick, Enzyme therapy. VI: Comparative in vivo fates and effects on lysosomal integrity of enzyme entrapped in negatively and positively charged liposomes, *Biochim. Biophys. Acta*, 1977, **464**(3), 530–546.

12 G. C. Reynolds, H. J. Baker and R. H. Reynolds, Enzyme replacement using liposome carriers in feline Gm1 gangliosidosis fibroblasts, *Nature*, 1978, **275**(5682), 754–755.

13 R. M. Haley, *et al.*, Lipid Nanoparticle Delivery of Small Proteins for Potent In Vivo RAS Inhibition, *ACS Appl. Mater. Interfaces*, 2023, **15**(18), 21877–21892.

14 Y. Fishman and N. Citri, L-asparaginase entrapped in liposomes: preparation and properties, *FEBS Lett.*, 1975, **60**(1), 17–20.

15 A. Sarkar, *et al.*, Cationic dextrin nanoparticles for effective intracellular delivery of cytochrome C in cancer therapy, *RSC Chem. Biol.*, 2024, **5**(3), 249–261.

16 G. N. Zhang, *et al.*, Lipid-Saporin Nanoparticles for the Intracellular Delivery of Cytotoxic Protein to Overcome ABC Transporter-Mediated Multidrug Resistance In Vitro and In Vivo, *Cancers*, 2020, **12**(2), 498.

17 P. Zhang, *et al.*, Lipo-Oligomer Nanoformulations for Targeted Intracellular Protein Delivery, *Biomacromolecules*, 2017, **18**(8), 2509–2520.

18 M. Wang, *et al.*, Combinatorially designed lipid-like nanoparticles for intracellular delivery of cytotoxic protein for cancer therapy, *Angew. Chem., Int. Ed.*, 2014, **53**(11), 2893–2898.

19 J. Kuhn, *et al.*, Delivery of Cas9/sgRNA Ribonucleoprotein Complexes via Hydroxystearyl Oligoamino Amides, *Bioconjugate Chem.*, 2020, **31**(3), 729–742.

20 J. Schulze, *et al.*, A Liposomal Platform for Delivery of a Protein Antigen to Langerin-Expressing Cells, *Biochemistry*, 2019, **58**(21), 2576–2580.

21 E. C. Wamhoff, *et al.*, A Specific, Glycomimetic Langerin Ligand for Human Langerhans Cell Targeting, *ACS Cent. Sci.*, 2019, **5**(5), 808–820.

22 B. E. Clausen and P. Stoitzner, Functional Specialization of Skin Dendritic Cell Subsets in Regulating T Cell Responses, *Front. Immunol.*, 2015, **6**, 534.

23 P. Stoitzner, *et al.*, Langerhans cells cross-present antigen derived from skin, *Proc. Natl. Acad. Sci. U. S. A.*, 2006, **103**(20), 7783–7788.

24 A. Kubo, *et al.*, External antigen uptake by Langerhans cells with reorganization of epidermal tight junction barriers, *J. Exp. Med.*, 2009, **206**(13), 2937–2946.

25 T. Vardam and N. Anandasabapathy, Langerhans Cells Orchestrate T(FH)-Dependent Humoral Immunity, *J. Invest. Dermatol.*, 2017, **137**(9), 1826–1828.

26 M. Rentzsch, *et al.*, Specific Protein Antigen Delivery to Human Langerhans Cells in Intact Skin, *Front. Immunol.*, 2021, **12**, 732298.

27 R. H. Liu, *et al.*, Passive mixing in a three-dimensional serpentine microchannel, *J. Microelectromech. Syst.*, 2000, **9**(2), 190–197.

28 C.-Y. Lee, *et al.*, Passive mixers in microfluidic systems: A review, *Chem. Eng. J.*, 2016, **288**, 146–160.

29 R. Tenchov, *et al.*, Lipid Nanoparticles—From Liposomes to mRNA Vaccine Delivery, a Landscape of Research Diversity and Advancement, *ACS Nano*, 2021, **15**(11), 16982–17015.

30 S. Pisani, *et al.*, Investigation and Comparison of Active and Passive Encapsulation Methods for Loading Proteins into Liposomes, *Int. J. Mol. Sci.*, 2023, **24**(17), 13542.

31 N. Forbes, *et al.*, Rapid and scale-independent microfluidic manufacture of liposomes entrapping protein incorporating in-line purification and at-line size monitoring, *Int. J. Pharm.*, 2019, **556**, 68–81.

32 V. Gogvadze, S. Orrenius and B. Zhivotovsky, Multiple pathways of cytochrome c release from mitochondria in apoptosis, *Biochim. Biophys. Acta*, 2006, **1757**(5–6), 639–647.

33 J. Hanske, *et al.*, Bacterial Polysaccharide Specificity of the Pattern Recognition Receptor Langerin Is Highly Species-dependent, *J. Biol. Chem.*, 2017, **292**(3), 862–871.

34 D. Alvarez-Paggi, *et al.*, Multifunctional Cytochrome c: Learning New Tricks from an Old Dog, *Chem. Rev.*, 2017, **117**(21), 13382–13460.

35 T. B. Gandek, L. van der Koog and A. Nagelkerke, A Comparison of Cellular Uptake Mechanisms, Delivery Efficacy, and Intracellular Fate between Liposomes and Extracellular Vesicles, *Adv. Healthc. Mater.*, 2023, **12**(25), e2300319.

36 S. Chatterjee, *et al.*, Endosomal escape: A bottleneck for LNP-mediated therapeutics, *Proc. Natl. Acad. Sci. U. S. A.*, 2024, **121**(11), e2307800120.

37 Y. Eygeris, *et al.*, Deconvoluting Lipid Nanoparticle Structure for Messenger RNA Delivery, *Nano Lett.*, 2020, **20**(6), 4543–4549.

38 M. Herrera, *et al.*, Illuminating endosomal escape of polymorphic lipid nanoparticles that boost mRNA delivery, *Biomater. Sci.*, 2021, **9**(12), 4289–4300.

39 H. Akita, Development of an SS-Cleavable pH-Activated Lipid-Like Material (ssPalm) as a Nucleic Acid Delivery Device, *Biol. Pharm. Bull.*, 2020, **43**(11), 1617–1625.

40 T. Doebel, B. Voisin and K. Nagao, Langerhans Cells - The Macrophage in Dendritic Cell Clothing, *Trends Immunol.*, 2017, **38**(11), 817–828.

41 D. P. Santana, *et al.*, Palladacycles catalyse the oxidation of critical thiols of the mitochondrial membrane proteins and lead to mitochondrial permeabilization and cytochrome c release associated with apoptosis, *Biochem. J.*, 2009, **417**(1), 247–256.

42 H. Feinberg, *et al.*, Structural basis for langerin recognition of diverse pathogen and mammalian glycans through a single binding site, *J. Mol. Biol.*, 2011, **405**(4), 1027–1039.

43 C. E. Allen, M. Merad and K. L. McClain, Langerhans-Cell Histiocytosis, *N. Engl. J. Med.*, 2018, **379**(9), 856–868.

44 F. Stirpe, *et al.*, Hepatotoxicity of immunotoxins made with saporin, a ribosome-inactivating protein from Saponaria officinalis, *Virchows Arch. B*, 1987, **53**(5), 259–271.

45 F. Giansanti, *et al.*, Strategies to Improve the Clinical Utility of Saporin-Based Targeted Toxins, *Toxins*, 2018, **10**(2), 82.

46 A. Kissenpfennig, *et al.*, Disruption of the langerin/CD207 gene abolishes Birbeck granules without a marked loss of Langerhans cell function, *Mol. Cell. Biol.*, 2005, **25**(1), 88–99.

47 A. Bobr, *et al.*, Acute ablation of Langerhans cells enhances skin immune responses, *J. Immunol.*, 2010, **185**(8), 4724–4728.

48 J. Wu, *et al.*, Challenges in delivering therapeutic peptides and proteins:A silk-based solution, *J. Controlled Release*, 2022, **345**, 176–189.

49 P. Tajpara, *et al.*, Epicutaneous administration of the pattern recognition receptor agonist polyinosinic-polycytidylic acid activates the MDA5/MAVS pathway in Langerhans cells, *FASEB J.*, 2018, **32**(8), 4132–4144.